Chapter 2

Heuristic Formulation of Time-Frequency Distributions[0]

Having established the basic signal formulations in the first chapter, we now turn to the problem of representing signals in a joint time-frequency domain. Given an analytic signal $z(t)$ obtained from a real signal $s(t)$, we seek to construct a time-frequency distribution $\rho_z(t,f)$ to represent precisely the energy, temporal and spectral characteristics of the signal. We choose the symbol ρ_z in the expectation that the TFD will represent an "energy density of z" in the (t,f) plane. We would also like the constant-t cross-section of $\rho_z(t,f)$ to be some sort of "instantaneous spectrum" at time t.

In this chapter we examine a variety of *ad hoc* approaches to the problem, namely the Wigner-Ville distribution (Section 2.1), a time-varying power spectral density called the Wigner-Ville Spectrum (2.2), localized forms of the Fourier Transform (2.3), filter banks (2.4), Page's instantaneous power spectrum (2.5), and related energy densities (2.6). Finally (in Section 2.7), we show how all these distributions are related to the first-mentioned Wigner-Ville distribution, thus setting the scene for the more systematic treatment in the next chapter.

The various distributions are illustrated using a linear FM asymptotic signal. The linear FM signal [Eq. (1.1.5)] is regarded as the most basic test signal for TFDs because it is the simplest example of a signal whose frequency content varies with time. It is clearly monocomponent, and is asymptotic if its BT product is large. The minimum requirement for a useful TFD is that it clearly shows the IF law of an asymptotic linear FM signal, giving a reasonable concentration of energy about the IF law (which, for an asymptotic signal, is equivalent to the TD law).

[0]Author: **Boualem Boashash**, Signal Processing Research Centre, Queensland University of Technology, Brisbane, Australia. Reviewers: K. Abed-Meraim, A. Beghdadi, M. Mesbah, G. Putland and V. Sucic.

2.1 Method 1: The Wigner-Ville Distribution

For a monocomponent signal, it is reasonable to expect that the TFD should take the form of a knife-edge ridge whose crest is a graph of the IF law in the (t, f) plane. Mathematically we idealize the "knife edge" as a delta function w.r.t. frequency.

2.1.1 Knife-Edge IF Indication

Noting that ρ_z is a function of frequency f and represents a kind of spectrum, we may reasonably require ρ_z to be the FT of some function related to the signal. Let us call this function the **signal kernel** and give it the symbol K_z. So the signal kernel can be written as $K_z(t,\tau)$, and the TFD is

$$\rho_z(t,f) = \underset{\tau\to f}{\mathcal{F}}\{K_z(t,\tau)\}. \tag{2.1.1}$$

2.1.2 Formulation of the Signal Kernel

To find a suitable form for $K_z(t,\tau)$, for simplicity, let us first consider the case of the unit-amplitude monocomponent FM signal

$$z(t) = e^{j\phi(t)} \tag{2.1.2}$$

whose instantaneous frequency is

$$f_i(t) = \frac{\phi'(t)}{2\pi}. \tag{2.1.3}$$

We would like the TFD of $z(t)$ at any given time to be a unit delta function at the instantaneous frequency, so that the "instantaneous spectrum" reduces to the ordinary Fourier transform in the constant-frequency case; that is, we want

$$\rho_z(t,f) = \delta(f - f_i(t)). \tag{2.1.4}$$

Substituting this into Eq. (2.1.1) and taking the IFT, we obtain

$$\begin{aligned} K_z(t,\tau) &= \underset{\tau\leftarrow f}{\mathcal{F}^{-1}}\left\{\delta(f - f_i(t))\right\} = e^{j2\pi f_i(t)\tau} \\ &= e^{j\phi'(t)\tau}. \end{aligned} \tag{2.1.5}$$

Because $\phi'(t)$ in Eq. (2.1.5) is not directly available, we write

$$\phi'(t) = \lim_{\tau\to 0} \frac{\phi(t+\frac{\tau}{2}) - \phi(t-\frac{\tau}{2})}{\tau}\ , \tag{2.1.6}$$

and use the approximation

$$\phi'(t) \approx \frac{1}{\tau}\left[\phi(t+\tfrac{\tau}{2}) - \phi(t-\tfrac{\tau}{2})\right] \tag{2.1.7}$$

which is called the **central finite-difference** (CFD) approximation [1, 2]. Substituting Eq. (2.1.7) into Eq. (2.1.5) and using Eq. (2.1.2) gives the signal kernel

$$\begin{aligned} K_z(t,\tau) &= e^{j\phi(t+\frac{\tau}{2})}\, e^{-j\phi(t-\frac{\tau}{2})} \\ &= z(t+\tfrac{\tau}{2})\, z^*(t-\tfrac{\tau}{2})\ . \end{aligned} \tag{2.1.8}$$

2.1.3 The Wigner Distribution

Substituting Eq. (2.1.8) into Eq. (2.1.1), we obtain

$$\rho_z(t,f) = \underset{\tau\to f}{\mathcal{F}}\left\{z(t+\tfrac{\tau}{2})\, z^*(t-\tfrac{\tau}{2})\right\} \tag{2.1.9}$$

$$= \int_{-\infty}^{\infty} z(t+\tfrac{\tau}{2})\, z^*(t-\tfrac{\tau}{2})\, e^{-j2\pi f\tau}\, d\tau. \tag{2.1.10}$$

Eq. (2.1.10) is given the symbol $\mathcal{W}_z(t,f)$, and is called the **Wigner distribution** (WD) in honor of its discoverer,[1] who derived it in 1932 in a quantum-mechanical context [3].

The approximation in Eq. (2.1.7) is exact if ϕ is a linear function of t, i.e. if $\phi'(t)$ is constant; it is also exact if $\phi(t)$ is quadratic [4, p. 298], i.e. if $\phi'(t)$ is linear. Thus the WD gives an "unbiased" estimate of the IF for a complex linear FM signal.

The constant-frequency real signal

$$s(t) = \cos 2\pi f_c t \tag{2.1.11}$$

leads to the signal kernel

$$\begin{aligned} K_s(t,\tau) &= s(t+\tfrac{\tau}{2})\, s(t-\tfrac{\tau}{2}) \\ &= \cos 2\pi f_c(t+\tfrac{\tau}{2})\, \cos 2\pi f_c(t-\tfrac{\tau}{2}) \\ &= \tfrac{1}{2}\cos 2\pi f_c\tau + \tfrac{1}{2}\cos 2\pi 2f_c t. \end{aligned} \tag{2.1.12}$$

Taking Fourier transforms w.r.t. τ gives the WD

$$\begin{aligned} \mathcal{W}_s(t,f) &= \tfrac{1}{4}\delta(f-f_c) + \tfrac{1}{4}\delta(f+f_c) \\ &\quad + \tfrac{1}{2}[\cos 2\pi 2f_c t]\, \delta(f). \end{aligned} \tag{2.1.13}$$

The terms in $\delta(f \mp f_c)$ are naturally expected and arise because $s(t)$ may be expressed as a sum of complex sinusoids at frequencies $\pm f_c$. The term in $\delta(f)$ is an artifact arising because the **nonlinearity** of the WD causes interaction between the positive- and negative-frequency terms.

[1] E. P. Wigner (1902–1995) was born in Hungary, studied chemical engineering in Germany and eventually settled in the United States, where he specialized in mathematical physics. He was a joint winner of the 1963 Nobel Prize for Physics for his many contributions to particle physics, including his law of conservation of parity and his work on the strong nuclear force.

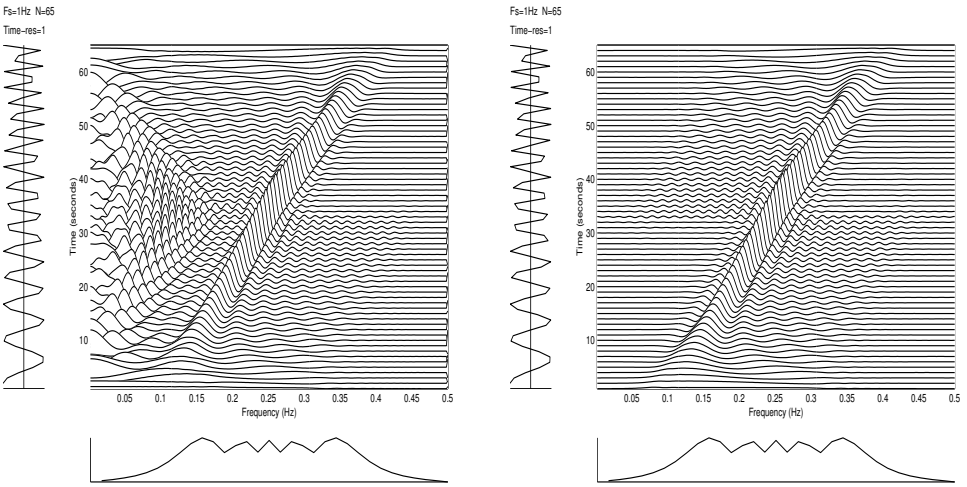

Fig. 2.1.1: Wigner distribution (left) and Wigner-Ville distribution (right) of a real linear FM signal [Eq. (1.1.5)] with duration 65 samples, starting frequency 0.1 and finishing frequency 0.4 (sampling rate 1 Hz). Note the low-frequency artifacts in the Wigner distribution, caused by interaction between positive and negative frequencies.

By a similar argument, we find that the non-windowed linear FM signal

$$s(t) = A\cos\left(2\pi[f_0 t + \tfrac{\alpha}{2}t^2]\right) \tag{2.1.14}$$

leads to the signal kernel

$$\begin{aligned} K_s(t,\tau) &= \tfrac{1}{2}A^2\cos 2\pi f_i(t)\tau \\ &\quad + \tfrac{1}{2}A^2\cos 2\pi\left[\tfrac{\alpha\tau^2}{4} + 2f_0 t + \alpha t^2\right] \end{aligned} \tag{2.1.15}$$

where $f_i(t) = f_0 + \alpha t$. Taking Fourier transforms w.r.t. τ gives the WD

$$\begin{aligned} \mathcal{W}_s(t,f) &= \tfrac{1}{4}A^2\delta(f - f_i(t)) + \tfrac{1}{4}A^2\delta(f + f_i(t)) \\ &\quad + \tfrac{1}{2}A^2 \underset{\tau\to f}{\mathcal{F}}\left\{\cos 2\pi\left[\tfrac{\alpha\tau^2}{4} + 2f_0 t + \alpha t^2\right]\right\}. \end{aligned} \tag{2.1.16}$$

The terms in $\delta(f \mp f_i(t))$ are naturally expected, while the last term in the signal kernel gives rise to a continuum of artifacts in the WD (see Fig. 2.1.1).

These artifacts, which greatly diminish the usefulness of the WD for real signals, are removed by modifying the WD with the analytic signal in accordance with the following.

2.1.4 The Wigner-Ville Distribution

Definition 2.1.1: *The* **Wigner-Ville distribution** *(***WVD***) of a signal $s(t)$, denoted by $W_z(t,f)$, is defined as the WD of its analytic associate, i.e.*

$$W_z(t,f) = \underset{\tau \to f}{\mathcal{F}} \left\{ z(t+\tfrac{\tau}{2})\, z^*(t-\tfrac{\tau}{2}) \right\} \tag{2.1.17}$$

where $z(t)$ is the analytic associate of $s(t)$.

The name "Wigner-*Ville* distribution", as opposed to "Wigner distribution", emphasizes the use of the analytic signal [5] and recognizes the contribution of Ville [6], who derived the distribution in a signal-processing context in 1948. Noting that a signal can have a time-dependent frequency content, Ville sought an "instantaneous spectrum" having the attributes of an energy density (property 1 in Section 1.1.5) and satisfying the so-called **marginal conditions**:[2]

- the integral of the TFD $\rho_z(t,f)$ w.r.t. frequency is the instantaneous power $|z(t)|^2$;
- the integral of the TFD $\rho_z(t,f)$ w.r.t. time is the energy spectrum $|Z(f)|^2$.

By analogy with the conditional moments of a p.d.f., and using known relationships between the moments of a p.d.f. and its characteristic function, Ville was able to show that the distribution now known as the WVD had the desired properties [7, pp. 946–7]. Using Eq. (2.1.8), we obtain

$$W_z(t,f) = \underset{\tau \to f}{\mathcal{F}} \{ K_z(t,\tau) \}. \tag{2.1.18}$$

The signal kernel $K_z(t,\tau)$ is also called the **instantaneous autocorrelation function** (IAF) of $z(t)$.

Furthermore, all TFDs in this Chapter, unless otherwise stated, are defined from the analytic associate of the signal, not from the real or "raw" signal.

2.1.4.1 The WVD of a Linear FM Signal

Eq. (2.1.2) describes a constant-amplitude, infinite-duration signal. We can allow for non-constant amplitude and finite duration using the form

$$z(t) = a(t)\, e^{j\phi(t)} \tag{2.1.19}$$

where $a(t)$ is real. For this signal we find

$$K_z(t,\tau) = K_a(t,\tau)\, e^{j\psi(t,\tau)} \tag{2.1.20}$$

[2] The name "marginal" can be explained with reference to the discrete-time, discrete-frequency case: if the TFD were written as a two dimensional array of discrete energies, each energy corresponding to a discrete time (vertical axis) and a discrete frequency (horizontal axis), then the sum over time for each frequency could be written in the horizontal "margin" of the array, and the sum over frequency for each time could be written in the vertical "margin".

where

$$K_a(t,\tau) = a(t+\tfrac{\tau}{2})\, a(t-\tfrac{\tau}{2}) \tag{2.1.21}$$

$$\psi(t,\tau) = \phi(t+\tfrac{\tau}{2}) - \phi(t-\tfrac{\tau}{2}). \tag{2.1.22}$$

If $\phi(t)$ is quadratic (i.e. if $f_i(t)$ is linear), then the CFD approximation is exact and gives $\psi(t,\tau) = \phi'(t)\tau = 2\pi f_i(t)\tau$, so that

$$K_z(t,\tau) = K_a(t,\tau)\, e^{j2\pi f_i(t)\tau}. \tag{2.1.23}$$

So $K_z(t,\tau)$, considered as a function of τ, has a constant frequency equal to $f_i(t)$; this reduction is called **dechirping**. If we let $\mathcal{W}_a(t,f) = \underset{\tau\to f}{\mathcal{F}}\{K_a(t,\tau)\}$, so that $\mathcal{W}_a(t,f)$ is the WD of $a(t)$, and take the FT of Eq. (2.1.23) w.r.t. τ, we obtain

$$W_z(t,f) \;=\; \mathcal{W}_a(t,f) \underset{f}{*} \delta(f - f_i(t)) \tag{2.1.24}$$

$$\;=\; \mathcal{W}_a(t, f - f_i(t)). \tag{2.1.25}$$

Now $K_a(t,\tau)$ is real and even in τ. Hence $\mathcal{W}_a(t,f)$ is real and even in f, so that $W_z(t,f)$ is real and symmetrical about $f = f_i(t)$.

Thus, even for a *finite*-duration linear FM signal, such as the one analyzed in Fig. 1.1.3, we expect the WVD to give a clear indication of the IF law. In fact, the TFD shown in Fig. 1.1.3 *is* the WVD of a finite duration linear FM signal.

2.1.4.2 The WVD in terms of the Spectrum

The variables t, f and τ are called time, frequency and lag, respectively. We now introduce the variable ν, which represents frequency *shift* just as τ represents time shift; accordingly, ν will be called **Doppler**.[3]

Let

$$k_z(\nu,f) = \underset{t\to\nu}{\mathcal{F}}\{W_z(t,f)\}. \tag{2.1.26}$$

Writing out the definitions of the FT and the WVD and taking invariant factors inside the integral signs, we obtain

$$k_z(\nu,f) = \iint z(t+\tfrac{\tau}{2})\, z^*(t-\tfrac{\tau}{2})\, e^{-j2\pi(f\tau+\nu t)} dt\, d\tau \tag{2.1.27}$$

where the integrals are from $-\infty$ to ∞. If we write

$$x = t + \tfrac{\tau}{2}\;; \quad y = t - \tfrac{\tau}{2} \tag{2.1.28}$$

and solve for t and τ, obtaining

$$t = \tfrac{1}{2}(x+y)\;; \quad \tau = x - y\;, \tag{2.1.29}$$

[3]The well-known "Doppler effect" is actually a frequency *scaling*. But when the effect is used to measure velocity, the scaling factor is usually close to unity and the bandwidth of interest is usually narrow. Under these conditions, the frequency scaling is well approximated by a frequency *shift* proportional to the velocity.

then the use of the Jacobian yields

$$dt\,d\tau = dx\,dy. \tag{2.1.30}$$

With these substitutions, we find that Eq. (2.1.27) can be factored into

$$\begin{aligned} k_z(\nu, f) &= \int_{-\infty}^{\infty} z(x)\, e^{-j2\pi[f+\nu/2]x} dx \cdot \int_{-\infty}^{\infty} z^*(y)\, e^{j2\pi[f-\nu/2]y} dy \\ &= Z(f+\tfrac{\nu}{2})\, Z^*(f-\tfrac{\nu}{2}) \end{aligned} \tag{2.1.31}$$

where $Z(f) = \mathcal{F}\{z(t)\}$. Noting that $k_z(\nu, f)$ has a similar form to $K_z(t, \tau)$ in the Doppler-frequency domain, we describe $k_z(\nu, f)$ as the "spectral autocorrelation function".

Substituting Eq. (2.1.31) into Eq. (2.1.26) and taking the IFT yields an expression for the WVD in terms of $Z(f)$:

$$W_z(t, f) = \int_{-\infty}^{\infty} Z(f+\tfrac{\nu}{2})\, Z^*(f-\tfrac{\nu}{2})\, e^{j2\pi\nu t} d\nu. \tag{2.1.32}$$

2.1.4.3 Effects of Time- and Frequency-Limiting

A practical signal $z(t)$ is often expected to be both time-limited and band-limited, despite theoretical constraints. Let us assume that $z(t)$ is windowed in both time and frequency.

For the time windowing, we can replace $z(t)$ by

$$z_w(t) = z(t)\, w(t - t_0). \tag{2.1.33}$$

The WVD of $z_w(t)$ is

$$W_{z_w}(t, f) = \int_{-\infty}^{\infty} z(t+\tfrac{\tau}{2})\, w(t-t_0+\tfrac{\tau}{2})\, z^*(t-\tfrac{\tau}{2})\, w^*(t-t_0-\tfrac{\tau}{2})\, e^{-j2\pi f\tau} d\tau. \tag{2.1.34}$$

Putting $t_0 = t$ gives

$$W_{z_w}(t, f) = \int_{-\infty}^{\infty} g_2(\tau)\, K_z(t, \tau)\, e^{-j2\pi f\tau} d\tau \tag{2.1.35}$$

where

$$g_2(\tau) = w(\tfrac{\tau}{2})\, w^*(-\tfrac{\tau}{2}). \tag{2.1.36}$$

If $g_2(\tau) = 0$ for $|\tau| > T/2$, then the limits of integration in Eq. (2.1.35) may be changed to $\pm T/2$. Notice that $W_{z_w}(t, f)$ differs from the WVD of $z(t)$ in that the IAF is multiplied by $g_2(\tau)$ before being Fourier-transformed w.r.t. τ. This $g_2(\tau)$ is thus the effective lag window corresponding to the sliding time window $w(t - t_0)$. For the frequency windowing, we can replace $Z(f)$ by

$$Z_H(f) = Z(f)\, H(f - f_0). \tag{2.1.37}$$

Using Eq. (2.1.32), we can take the WVD corresponding to $Z_H(f)$ and put $f_0 = f$, obtaining in a similar manner to the above:

$$W_{Z_H}(t,f) = \int_{-\infty}^{\infty} G_1(\nu)\, Z(f+\tfrac{\nu}{2})\, Z^*(f-\tfrac{\nu}{2})\, e^{j2\pi\nu t} d\nu \tag{2.1.38}$$

where

$$G_1(\nu) = H(\tfrac{\nu}{2})\, H^*(-\tfrac{\nu}{2}). \tag{2.1.39}$$

If $G_1(\nu) = 0$ for $|\nu| > B/2$, then the limits of integration in Eq. (2.1.38) may be changed to $\pm B/2$. Notice that $W_{Z_H}(t,f)$ differs from the WVD of $z(t)$ in that the spectral autocorrelation function is multiplied by $G_1(\nu)$ before being inverse-Fourier-transformed w.r.t. ν. This $G_1(\nu)$ is the effective Doppler window corresponding to the sliding frequency window $H(f-f_0)$.

The effects of time windowing and frequency windowing may be combined as multiplication by the factor

$$g(\nu,\tau) = G_1(\nu)\, g_2(\tau) \tag{2.1.40}$$

in the (ν,τ) domain. If we consider time-limiting alone, the resulting TFD is given by Eq. (2.1.35) and is called the **windowed WVD** [8–10]. If we consider band-limiting alone, the resulting TFD is given by Eq. (2.1.38). We shall call this the **filtered WVD**. The window shapes of G_1 and g_2 should be selected to ensure the properties 1 to 3 in Section 1.1.5 are verified.

2.2 Method 2: Time-Varying Power Spectral Density

2.2.1 Spectra of Non-Stationary Random Processes

If $z(t)$ is a complex random signal, its symmetrical **autocorrelation** function is defined as

$$\mathcal{R}_z(t,\tau) = \mathcal{E}\big\{z(t+\tfrac{\tau}{2})\, z^*(t-\tfrac{\tau}{2})\big\} \tag{2.2.1}$$

where $\mathcal{E}\{\ldots\}$ denotes the expected value. If $z(t)$ is wide-sense stationary, then $\mathcal{R}_z(t,\tau)$ is independent of t, and the limit

$$\mathcal{S}_z(f) \stackrel{\triangle}{=} \lim_{T\to\infty} \mathcal{E}\left\{\frac{1}{T}\left|\underset{t\to f}{\mathcal{F}}\{z(t)\ \mathrm{rect}(t/T)\}\right|^2\right\} \tag{2.2.2}$$

is called the **power spectral density** (**PSD**) of the random process $z(t)$, and describes the distribution of signal power over the frequencies. The PSD is related to the autocorrelation function by the **Wiener-Khintchine theorem**, which states that

$$\mathcal{S}_z(f) = \underset{\tau\to f}{\mathcal{F}}\{\mathcal{R}_z(t,\tau)\}. \tag{2.2.3}$$

If $z(t)$ is not wide-sense stationary, the right-hand side of this equation depends on t, so that the left-hand side also depends on t, suggesting the generalization

$$\mathcal{S}_z(t,f) \stackrel{\triangle}{=} \underset{\tau\to f}{\mathcal{F}}\{\mathcal{R}_z(t,\tau)\}. \tag{2.2.4}$$

This $\mathcal{S}(t,f)$ may be called the time-varying spectrum or **evolutive spectrum** (ES), and is interpreted as the "time-dependent PSD" of the non-stationary signal. The right-hand side of Eq. (2.2.4) may be expanded as

$$\begin{aligned}
\underset{\tau\to f}{\mathcal{F}}\{\mathcal{R}_z(t,\tau)\} &= \int_{-\infty}^{\infty} \mathcal{E}\left\{z(t+\tfrac{\tau}{2})\, z^*(t-\tfrac{\tau}{2})\right\} e^{-j2\pi f\tau} d\tau && (2.2.5)\\
&= \mathcal{E}\left\{\int_{-\infty}^{\infty} z(t+\tfrac{\tau}{2})\, z^*(t-\tfrac{\tau}{2}) e^{-j2\pi f\tau} d\tau\right\} && (2.2.6)\\
\mathcal{S}_z(t,f) &= \mathcal{E}\{W_z(t,f)\}\,. && (2.2.7)
\end{aligned}$$

Eq. (2.2.7) shows that the expected value of the WVD is the FT of the time-dependent autocorrelation function [11]; that is, the ES is the expected value of the WVD. For this reason, the ES is also called the **Wigner-Ville spectrum**.

If $z(t)$ is deterministic, Eq. (2.2.7) reduces to

$$\mathcal{S}_z(t,f) = W_z(t,f). \tag{2.2.8}$$

2.2.2 Estimating the Wigner-Ville Spectrum

Eq. (2.2.7) refers to an ensemble average of the random process $W_z(t,f)$. If we have only one realization of this process, we may be able to assume that $W_z(\theta,f)$ is locally ergodic on the interval $t-\Delta/2<\theta<t+\Delta/2$, where Δ is positive and independent of t. First we calculate an estimate of $W_z(t,f)$ for the local values of $z(t)$, yielding

$$\begin{aligned}
\widehat{W}_z(t,f) &= \underset{\tau\to f}{\mathcal{F}}\{g_2(\tau)\, K_z(t,\tau)\} && (2.2.9)\\
&= G_2(f) \underset{f}{*} W_z(t,f) && (2.2.10)
\end{aligned}$$

where $g_2(\tau)$, the effective analysis window, is real, even and time-limited, and $G_2(f)=\mathcal{F}\{g_2(\tau)\}$.

Then, to obtain an estimate of $\mathcal{S}_z(t,f)$, we replace the ensemble average over all realizations of $W_z(t,f)$ by a time average of $\widehat{W}_z(t,f)$ over the interval Δ. We can calculate such an average using a real, even weighting function $g_1(t)$, with the properties

$$g_1(t) \begin{cases} >0 & \text{if } |t|\le\Delta/2 \\ =0 & \text{otherwise} \end{cases} \tag{2.2.11}$$

$$\int_{-\infty}^{\infty} g_1(t)\, dt = 1\ . \tag{2.2.12}$$

The resulting estimate of $\mathcal{S}_z(t,f)$ is

$$\widehat{\mathcal{S}}_z(t,f) = \int_{-\infty}^{\infty} g_1(\theta - t)\, \widehat{W}_z(\theta, f)\, d\theta. \tag{2.2.13}$$

Using the evenness of g_1 and substituting from Eq. (2.2.10), we have

$$\widehat{\mathcal{S}}_z(t,f) = g_1(t) \underset{t}{*} \widehat{W}_z(t,f) = g_1(t) \underset{t}{*} G_2(f) \underset{f}{*} W_z(t,f). \tag{2.2.14}$$

This can be written

$$\widehat{\mathcal{S}}_z(t,f) = \gamma(t,f) \underset{(t,f)}{**} W_z(t,f) \tag{2.2.15}$$

where

$$\gamma(t,f) = g_1(t)\, G_2(f) \tag{2.2.16}$$

and the double asterisk denotes **double convolution**.

Eq. (2.2.15) defines a class of estimates for time-varying spectra obtained by a double convolution of the WVD with a 2D filter. This will be used in the next chapter to define quadratic TFDs with specific properties.

2.3 Method 3: Windowed Fourier Transform (STFT, Spectrogram & Gabor Transform)

2.3.1 STFT and Spectrogram

Consider a signal $s(\tau)$ and a real, even window $w(\tau)$, whose FTs are $S(f)$ and $W(f)$ respectively. To obtain a localized spectrum of $s(\tau)$ at time $\tau = t$, multiply the signal by the window $w(\tau)$ centered at time $\tau = t$, obtaining

$$s_w(t,\tau) = s(\tau)\, w(\tau - t)\ , \tag{2.3.1}$$

and then take the FT w.r.t. τ, obtaining

$$F_s^w(t,f) = \underset{\tau \to f}{\mathcal{F}} \{ s(\tau)\, w(\tau - t) \}. \tag{2.3.2}$$

$F_s^w(t,f)$ is called the **short-time Fourier transform** (**STFT**).

The squared magnitude of the STFT, denoted by $S_s^w(t,f)$, is called the **spectrogram**:

$$S_s^w(t,f) = |F_s^w(t,f)|^2 \tag{2.3.3}$$

$$= \left| \underset{\tau \to f}{\mathcal{F}} \{ s(\tau)\, w(\tau - t) \} \right|^2 \tag{2.3.4}$$

$$= \left| \int_{-\infty}^{\infty} s(\tau)\, w(\tau - t)\, e^{-j2\pi f \tau} d\tau \right|^2 . \tag{2.3.5}$$

In the notation $S_s^w(t,f)$, the upper-case S stands for "spectrogram", while the subscript stands for the signal and the superscript for the filter.

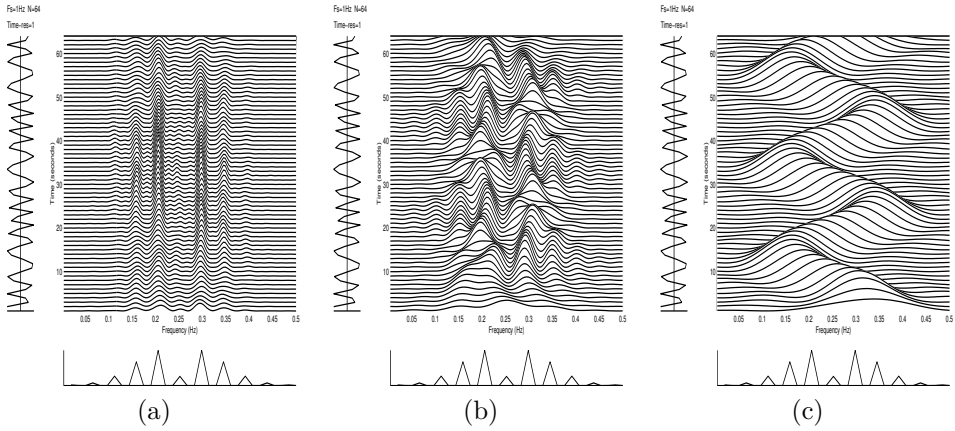

Fig. 2.3.1: Spectrogram of a sinusoidal FM signal [Eq. (1.1.4)] with 65 samples (sampling rate 1 Hz), $A = 1$, $f_c = 1/4$, $f_m = 3/64$, $f_d = 6/64$, rectangular window of length Δ samples: (a) $\Delta = 63$; (b) $\Delta = 23$; (c) $\Delta = 7$.

The observation window $w(\tau)$ allows localization of the spectrum in time, but also smears the spectrum in frequency[4] in accordance with the "uncertainty relationship" [12], leading to a trade-off between time resolution and frequency resolution. The problem is illustrated in Fig. 2.3.1, which shows the spectrogram of a sinusoidal FM signal for a rectangular window of three different lengths. If the window is long compared with the modulating signal, the frequency resolution is sufficient to show the sideband tones (the "multicomponent aspect" [13] of the signal), but the time resolution is insufficient to show the FM law (the "monocomponent aspect"). If the window is short compared with the modulating signal, the time resolution is sufficient to show the FM law but the frequency resolution is insufficient to show the sideband tones.

The spectrogram is nonlinear; but the nonlinearity is introduced only in the final step (taking the squared magnitude) and therefore does not lead to undesirable artifacts present in other TFDs. This freedom from artifacts, together with simplicity, robustness and ease of interpretation, has made the spectrogram a popular tool for speech analysis (resolution of speech into phonemes and formants) since its invention in 1946 [14].

2.3.2 Optimal Window Length of the Spectrogram

The spectrogram involves a compromise between time resolution and frequency resolution: a longer window provides less localization in time and more discrimination in frequency.

[4] **Smearing** is caused by the convolution operation. If an image (a function of two coordinates) is convolved with a confusion pattern (another function of the same two coordinates), the result is a blurred image. If the confusion pattern is a line, we tend to describe the blurring as a "smearing".

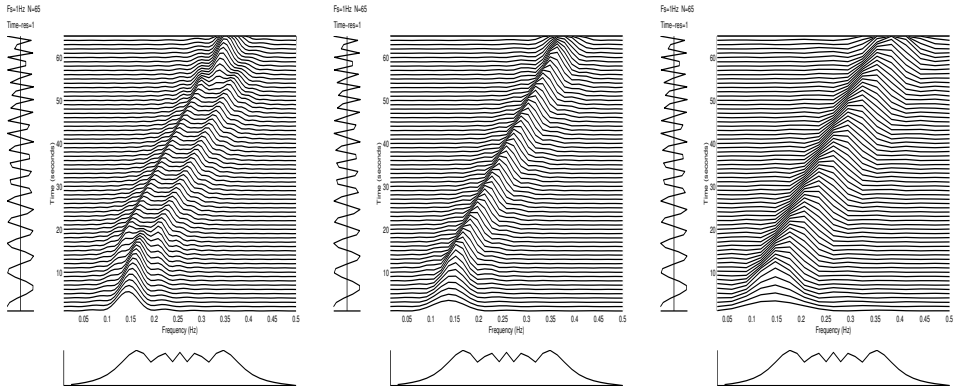

Fig. 2.3.2: Spectrogram of a linear FM signal [Eq. (1.1.5)] with duration 65, starting frequency 0.1 and finishing frequency 0.4, for a rectangular window of length Δ: (a) $\Delta = 33$; (b) $\Delta = 21$; (c) $\Delta = 11$. The optimal window length according to Eq. (2.3.6) is 20.7.

The purpose of the window is to obtain a time-slice of the signal during which the spectral characteristics are nearly constant. If the window is too long, it fails to capture the most rapid variations of spectral content. If it is too short, it smears the TFD in the frequency dimension without a commensurate improvement in detail in the time dimension. The more rapidly the spectral content changes, the shorter the window must be.

Hence, for a monocomponent signal of constant amplitude, the optimal window duration is inversely related to the rate of change of the IF. More precisely, if the window is rectangular and has total duration Δ, it can be shown [15, 16] that the value

$$\Delta = \sqrt{2} \left| \frac{df_i(t)}{dt} \right|^{-1/2} \tag{2.3.6}$$

is optimal in the sense that it minimizes the half-height width of the resulting ridge in the (t, f) plane. This optimal Δ is proportional to the relaxation time T_{r} ; compare it with Eq. (1.3.44). For a linear FM signal, the optimal window duration simplifies to $\Delta = \sqrt{2T/B}$, where T is the signal duration and B is the signal bandwidth [17]. Fig. 2.3.2 shows the spectrogram of a chirp signal (the same signal as in Fig. 1.1.3) for a rectangular window of three different lengths, one of which ($\Delta = 21$) is optimal according to Eq. (2.3.6).

Even for the optimal window length, the spectrogram is not a delta function describing the IF law. The use of this optimal window is inconvenient because it requires knowledge of the IF, and this knowledge might be obtainable only by some sort of time-frequency analysis. Moreover, if the IF law is nonlinear, the optimal window duration varies with time. In the case of the sinusoid FM signal of Fig. 2.3.1, the optimal window length is time-varying if the signal is considered as a modulated

carrier. Although it is possible to vary the spectrogram window length with time and even with frequency, such procedures have a cost in computational efficiency [18]. A recent iterative algorithm for matching the spectrogram window to the estimated IF, so that the spectrogram of a monocomponent signal is concentrated along the IF law, is described in [19] and in Article 10.1.

2.3.3 STFT vs. Gabor Transform

In 1946, while studying the requirements for efficient signal transmission, Gabor [12] noted that the (t, f) plane can be divided into an array of rectangles using a bank of filters, each of which is switched on for a single interval of time and passes a single band of frequencies. Each rectangle was called a **logon**, and its dimensions were called the **decay time** and the **tuning width**. Gabor noted that the dimensions must satisfy the Heisenberg uncertainty relation

$$\Delta t \Delta f \geq \frac{1}{4\pi} \tag{2.3.7}$$

where Δt and Δf are the effective duration and bandwidth of the logon [12]. Gabor showed this relationship to be "at the root of the fundamental principle of communication" [12], in that it puts a lower limit on the spread of a signal in time and frequency.[5] For the minimum elemental area, which is obtained in the case of a complex Gaussian signal, Eq. (2.3.7) becomes an equality as in Eq. (1.2.34).

In Gabor's representation, each logon is assigned a complex coefficient $c_{n,k}$, where n is the time index and k the frequency index. The signal $s(t)$ is expanded in the doubly infinite series

$$s(t) = \sum_{n,k} c_{n,k}\, \psi_{n,k}(t) \tag{2.3.8}$$

where the sum is over all integers n and k, and $\psi_{n,k}(t)$ is a function centered about time $n\Delta t$ and frequency $k\Delta f$. To find the coefficients $c_{n,k}$, let $h_{n,k}(t)$ and $\psi_{n,k}(t)$ be related by

$$\int_{-\infty}^{\infty} h^*_{m,l}(t)\, \psi_{n,k}(t)\, dt = \begin{cases} 1 & \text{if } m=n \text{ and } l=k\ ; \\ 0 & \text{otherwise}\ . \end{cases} \tag{2.3.9}$$

[5] Eq. (2.3.7) is perhaps best known for its corollary in quantum mechanics. If we write x (position) for t, and k (wave number) for $2\pi f$, we obtain

$$\Delta x \Delta k \geq 1/2.$$

De Broglie's "matter wave" relation may be written $k = 2\pi p/h$, where p is the momentum and h is Planck's constant. Making this substitution for k in the above equation, we obtain

$$\Delta x \Delta p \geq \frac{h}{4\pi}\ ,$$

which, for some readers, will be more familiar than Eq. (2.3.7).

In other words, let $h_{m,l}(t)$ be orthogonal to every $\psi_{n,k}(t)$ except $\psi_{m,l}(t)$, or, equivalently, let $\psi_{m,l}(t)$ be orthogonal to every $h_{n,k}(t)$ except $h_{m,l}(t)$; functions related in this way are called **dual functions**. Multiplying Eq. (2.3.8) by $h^*_{m,l}(t)$ and integrating w.r.t. t, we obtain an expression for $c_{n,k}$:

$$c_{n,k} = \int_{-\infty}^{\infty} s(\tau)\, h^*_{n,k}(\tau)\, d\tau. \tag{2.3.10}$$

If we choose

$$h_{n,k}(\tau) = w(\tau - n\Delta t)\, e^{j2\pi k\Delta f \tau} \tag{2.3.11}$$

where w denotes a real Gaussian function, then Eq. (2.3.10) becomes

$$c_{n,k} = \int_{-\infty}^{\infty} s(\tau)\, w(\tau - n\Delta t)\, e^{-j2\pi k\Delta f \tau} d\tau \tag{2.3.12}$$

$$= \underset{\tau \to k\Delta f}{\mathcal{F}} \{s(\tau)\, w(\tau - n\Delta t)\}. \tag{2.3.13}$$

Expression (2.3.13) is known as the **Gabor transform**. When $\psi_{n,k}(t)$ is chosen as the dual function of $h_{n,k}(t)$, Eq. (2.3.8) gives the **inverse Gabor transform**. Eq. (2.3.13) has the same form as Eq. (2.3.2) except that t and f are discretized, wherefore the Gabor transform has been described as a sampled STFT. Suitable selections of ψ and h need to be made for the TFD to verify the properties 1 to 3 in Section 1.1.5, at least approximately.

Lerner [20] extended Gabor's work by allowing the elements of the (t, f) plane to be non-rectangular. Helstrom [21] generalized the expansion by replacing the discrete elementary cell weighting with a continuous function $\xi(\tau, t, f)$. Wavelet theory [22] was developed later as a further extension of Gabor's work, but choosing the partitions of the (t, f) plane so as to give constant-Q filtering [23, 24].

2.4 Method 4: Filtered Function of Time

2.4.1 Filter Banks and the Sonograph

Whereas the spectrogram is conceived as a function of frequency with dependence on the timing of a window, the sonograph is conceived as a function of time with dependence on the tuning of a filter. Consider a signal $s(t)$ with spectrum $S(\nu)$, and a lowpass filter with the real impulse response $h(t)$ and the transfer function $H(\nu)$. To extract the bandpass "component" of $s(t)$ at frequency $\nu = f$, we shift the filter function in frequency so that it is centered at $\nu = f$, multiply the signal spectrum by the shifted filter function, and take the inverse FT w.r.t. ν, obtaining

$$B^H_s(t, f) = \underset{t \leftarrow \nu}{\mathcal{F}^{-1}} \{S(\nu)\, H(\nu - f)\} \tag{2.4.1}$$

where the "B" stands for "bandpass". This signal may be understood as the complex output of a bandpass filter with center frequency $+f$; the input $s(t)$ may be reconstructed as the sum of the outputs of such **filter banks** whose transfer functions add up to unity within the bandwidth of $s(t)$.

The squared magnitude of $B_s^H(t,f)$ is denoted by $S_s^{(H)}(t,f)$ and is called the **sonograph** or **sonogram**:

$$S_s^{(H)}(t,f) = |B_s^H(t,f)|^2 \tag{2.4.2}$$

$$= \left| \mathcal{F}^{-1}_{t\leftarrow\nu} \{S(\nu)\, H(\nu - f)\} \right|^2 \tag{2.4.3}$$

$$= \left| \int_{-\infty}^{\infty} S(\nu)\, H(\nu - f)\, e^{j2\pi\nu t} d\nu \right|^2 . \tag{2.4.4}$$

For the sonograph, the optimal bandwidth of the band-pass filter is related to the time delay in the same way that the optimal window length for the spectrogram is related to the instantaneous frequency.

Like the spectrogram, the sonograph is nonlinear, but the nonlinearity is introduced only in the final step and does not lead to artifacts. Filter banks—the practical realization of the sonograph—have long been used in music broadcasting, recording and even home entertainment, although the frequency division is not necessarily linear; for example, graphic equalizers and analyzers usually have logarithmic frequency division.

2.4.2 Equivalence to Spectrogram

Theorem 2.4.1: *The spectrogram and sonograph are equal if the window function of the spectrogram is real and even and equal to the impulse response of the sonograph filter for* $f = 0$ *.*

Proof: Applying the inverse convolution property to Eq. (2.4.1), we obtain

$$B_s^H(t,f) = s(t) \underset{t}{*} h(t) e^{j2\pi f t} \tag{2.4.5}$$

$$= \int_{-\infty}^{\infty} s(\tau)\, h(t-\tau)\, e^{j2\pi f (t-\tau)} d\tau \tag{2.4.6}$$

$$= e^{j2\pi f t} \underset{\tau\to f}{\mathcal{F}} \{s(\tau)\, h(t-\tau)\} \tag{2.4.7}$$

which yields

$$S_s^{(H)}(t,f) = \left| \underset{\tau\to f}{\mathcal{F}} \{s(\tau)\, h(t-\tau)\} \right|^2 . \tag{2.4.8}$$

Comparing Eqs. (2.3.4) and (2.4.8), we see that the spectrogram and sonograph are the same if

$$h(t) = w(-t) \ , \tag{2.4.9}$$

which is the case if $w(t)$ is even and equal to $h(t)$. The condition that $w(t)$ be real is redundant in the proof, but is assumed in the definition of the spectrogram. ■

2.5 Method 5: Instantaneous Power Spectra

2.5.1 Page Distribution

This approach attempts to define a kind of "running spectrum" by considering the variations of the signal spectrum as time t increases.

Given a signal $s(t)$, let us define the **running transform** $S_-(t,f)$ as the FT of the signal s up to time t. To do this, we first define the "auxiliary signal" $s_t(\theta)$ as

$$s_t(\theta) = \begin{cases} s(\theta) & \text{if } \theta \le t \\ 0 & \text{if } \theta > t \end{cases}. \tag{2.5.1}$$

Then the running transform is simply

$$S_-(t,f) = \underset{\theta\to f}{\mathcal{F}}\{s_t(\theta)\} = \int_{-\infty}^{t} s(\theta)\, e^{-j2\pi f\theta} d\theta. \tag{2.5.2}$$

As the normal energy spectrum is the squared magnitude of the FT, so the **running energy spectrum** up to time t, denoted by $e_s(t,f)$, is the squared magnitude of the running transform:

$$e_s(t,f) = |S_-(t,f)|^2 = S_-(t,f)\, S_-^*(t,f). \tag{2.5.3}$$

Differentiating each expression in this equation w.r.t. time, and denoting the time-derivative of $e_s(t,f)$ by $\mathrm{P}_s(t,f)$, we obtain

$$\mathrm{P}_s(t,f) \;=\; \frac{\partial}{\partial t}\Big[|S_-(t,f)|^2\Big] \tag{2.5.4}$$

$$\;=\; S_-(t,f)\,\frac{\partial}{\partial t}\big[S_-^*(t,f)\big] \;+\; S_-^*(t,f)\,\frac{\partial}{\partial t}[S_-(t,f)]\,. \tag{2.5.5}$$

This $\mathrm{P}_s(t,f)$, being the time-derivative of a time-dependent energy spectrum, may be understood as a kind of *time-dependent power spectrum*. It is now known as the **Page distribution** in honor of its discoverer [25].

By substituting the right-hand expression of Eq. (2.5.2) into Eq. (2.5.4), we obtain

$$\mathrm{P}_s(t,f) = \frac{\partial}{\partial t}\left[\left|\int_{-\infty}^{t} s(\theta)\, e^{-j2\pi f\theta} d\theta\right|^2\right] \tag{2.5.6}$$

which is the usual definition of the Page distribution. Using Eq. (2.5.2) to evaluate the partial derivatives in Eq. (2.5.5), we obtain the alternative expression

$$\mathrm{P}_s(t,f) = 2\,\mathrm{Re}\big\{s^*(t)\, S_-(t,f)\, e^{j2\pi ft}\big\} \tag{2.5.7}$$

or, substituting from Eq. (2.5.2) and writing $\tau = t-\theta$,

$$\mathrm{P}_s(t,f) = 2\,\mathrm{Re}\left\{\int_0^{\infty} s^*(t)\, s(t-\tau)\, e^{j2\pi f\tau}\, d\tau\right\}. \tag{2.5.8}$$

If $s(t)$ is real as Page assumed [25], Eq. (2.5.8) becomes

$$\mathrm{P}_s(t,f) = 2\int_0^{\infty} s(t)\, s(t-\tau)\cos(2\pi f\tau)\, d\tau. \tag{2.5.9}$$

The Page distribution of a time-limited linear FM signal is shown in Fig. 2.7.1(c). Notice that the distribution can take *negative values*, which are inconsistent with the notion of an energy *distribution*, but perfectly consistent with the notion of an energy *gradient* as defined in Eq. (2.5.6). As negative values compensate for earlier spurious positive values caused by the truncation of $s(t)$ to produce $s_t(\theta)$, the presence of negative values implies that energy is delocalized in the (t, f) domain.

2.6 Method 6: Energy Density

2.6.1 Rihaczek's Complex Energy Density

In search of a TFD localized in both time and frequency, Rihaczek [26] considered the energy of a complex deterministic signal over finite ranges of t and f, and allowed those ranges to become infinitesimal, obtaining what he called a **complex energy density**.

Here we offer a simpler derivation than that given by Rihaczek. The energy of a complex signal $z(t)$, with Fourier transform $Z(f)$, is

$$\begin{aligned} E &= \int_{-\infty}^{\infty} |z(t)|^2 dt = \int_{-\infty}^{\infty} z(t)\, z^*(t)\, dt = \int_{-\infty}^{\infty} z(t) \int_{-\infty}^{\infty} Z^*(f)\, e^{-j2\pi ft} df\, dt \\ &= \int_{-\infty}^{\infty}\int_{-\infty}^{\infty} \mathrm{R}_z(t, f)\, dt\, df \end{aligned} \tag{2.6.1}$$

where $\mathrm{R}_z(t, f)$, the energy density function, is defined by

$$\mathrm{R}_z(t, f) = z(t)\, Z^*(f)\, e^{-j2\pi ft}. \tag{2.6.2}$$

This $\mathrm{R}_z(t, f)$ is the **Rihaczek distribution** (RD). If we express $Z(f)$ and hence $Z^*(f)$ in terms of $z(\lambda)$ and use the substitution $\tau = t - \lambda$, we obtain the alternative form

$$\mathrm{R}_z(t, f) = \int_{-\infty}^{\infty} z(t)\, z^*(t - \tau)\, e^{-j2\pi f\tau} d\tau. \tag{2.6.3}$$

A distribution equivalent to Rihaczek's was derived earlier, in the context of quantum mechanics, by J. G. Kirkwood [27], so that the RD is also called the **Kirkwood-Rihaczek distribution** [28, p. 26].

From Eq. (2.6.2) it is easily verified that

$$\int_{-\infty}^{\infty} \mathrm{R}_z(t, f)\, df = |z(t)|^2 \tag{2.6.4}$$

$$\int_{-\infty}^{\infty} \mathrm{R}_z(t, f)\, dt = |Z(f)|^2. \tag{2.6.5}$$

That is, the RD satisfies the **marginal conditions** [see the discussion following Eq. (2.1.17)].

Integrating Eq. (2.6.4) w.r.t. t and Eq. (2.6.5) w.r.t. f, we obtain respectively

$$\int_{t_1}^{t_2}\int_{-\infty}^{\infty} \mathrm{R}_z(t,f)\,df\,dt = \int_{t_1}^{t_2} |z(t)|^2 dt \tag{2.6.6}$$

$$\int_{f_1}^{f_2}\int_{-\infty}^{\infty} \mathrm{R}_z(t,f)\,dt\,df = \int_{f_1}^{f_2} |Z(f)|^2 df. \tag{2.6.7}$$

The right-hand side of Eq. (2.6.6) is the energy in the time interval between t_1 and t_2, while the right-hand side of Eq. (2.6.7) is the energy in the frequency band between f_1 and f_2. Together, the two equations indicate that $\mathrm{R}_z(t,f)$ can be interpreted as an energy density over an arbitrary time interval *and* an arbitrary frequency band.

In Eq. (2.6.2), the RD has the signal $z(t)$ as a factor. It follows that the RD is zero at those times when $z(t)$ is zero; this property is called **strong time support**. Similarly we see that the RD is zero at those frequencies for which the spectrum $Z(f)$ is zero; this property is called **strong frequency support**.

2.6.2 Levin's Real Energy Density

The **Levin distribution** (**LD**) is simply the *real part* of the RD. It follows that the LD, like the RD, has strong time support and strong frequency support. Taking the real parts of Eqs. (2.6.4) to (2.6.5), we further conclude that the LD satisfies the marginal conditions and their corollaries.

Let the LD of the complex signal $z(t)$ be denoted by $\mathrm{L}_z(t,f)$. Taking the real part of Eq. (2.6.2), we obtain the definition

$$\mathrm{L}_z(t,f) = \mathrm{Re}\big\{ z(t)\, Z^*(f)\, e^{-j2\pi ft} \big\}. \tag{2.6.8}$$

Taking the real part of Eq. (2.6.3) yields the alternative expression

$$\mathrm{L}_z(t,f) = \mathrm{Re}\left\{ \int_{-\infty}^{\infty} z(t)\, z^*(t-\tau)\, e^{-j2\pi f\tau} d\tau \right\}. \tag{2.6.9}$$

If $z(t)$ is replaced by a real signal $s(t)$, Eq. (2.6.9) reduces to the cosine form obtained by Levin [29].

Historically, the distribution obtained by Levin was a modification of the Page distribution and a precursor of the RD. But it was first discovered in a quantum-mechanical context by Margenau and Hill [30]; so it is also called the **Margenau-Hill distribution** [28, p. 26].

2.6.3 Windowed Rihaczek and Levin Distributions

Because energy is a real quantity, the real part of the RD is more significant than the imaginary part or the magnitude. Hence a "plot of the RD" is usually a plot of the real part, i.e. the LD. Fig. 2.7.1(d) shows such a plot for a time-limited linear

FM signal. Although Eqs. (2.6.6) and (2.6.7) indicate that the energy of the TFD is well localized in the time and frequency dimensions separately, i.e. in strips parallel to the f and t axes, it does not follow that the energy is well localized in both dimensions at once. Indeed Fig. 2.7.1(d) shows that the peaks of the TFD are not confined to the IF law, but show many spurious features. The WVD of this signal [Fig. 2.7.1(a)] is much cleaner. Because the RD/LD performs so poorly on such a simple signal, it must be regarded as only of theoretical interest.

By comparison with the RD, the spectrogram is remarkably free of artifacts. Recall that the spectrogram is the squared magnitude of the STFT. So one way to reduce artifacts in the RD is to introduce the STFT as a factor [31] instead of the spectrum $Z(f)$, in Eq. (2.6.2). The resulting distribution, which might be called the **windowed Rihaczek distribution**, is

$$\rho_z(t,f) = z(t)\Big[\underset{\tau\to f}{\mathcal{F}}\{z(\tau)\,w(\tau-t)\}\Big]^*\,e^{-j2\pi ft} \tag{2.6.10}$$

where w is the window function of the STFT. As the real part of the RD is the LD, we might as well designate the real part of the windowed RD as the **windowed Levin distribution**. A windowed LD of a time-limited linear FM signal is shown in Fig. 2.7.1(e); note the reduction in artifacts compared with the conventional LD.

From the form of Eq. (2.6.10), we see that the windowed RD and the windowed LD have strong time support. Other properties of these distributions will emerge in later sections.

2.7 Relationship between TFDs

So far, we have considered six different approaches to defining a TFD. All the approaches seem natural and reasonable, and yet lead paradoxically to at least five different definitions of a TFD, all of them *quadratic* in the signal. Using the "signal kernel" approach [Eq. (2.1.1)], we may write for any TFD $\rho_z(t,f)$:

$$\rho_z(t,f) = \underset{\tau\to f}{\mathcal{F}}\{R_z(t,\tau)\}. \tag{2.7.1}$$

where $R_z(t,\tau)$ is found simply by taking the inverse FT of $\rho_z(t,f)$ w.r.t. f. In the case of the WVD, $R_z(t,\tau)$ is the instantaneous autocorrelation function (IAF), denoted by $K_z(t,\tau)$. In other cases we shall call $R_z(t,\tau)$ the **smoothed IAF**. The reason for this term will become apparent as we relate $R_z(t,\tau)$ to $K_z(t,\tau)$ for each of the TFDs that we have defined.

2.7.1 Spectrogram

From Eq. (2.3.4), the spectrogram with window function w can be rewritten in the generalized notation as

$$\rho_z(t,f) = \underset{\tau\to f}{\mathcal{F}}\{z(\tau)\,w(\tau-t)\}\,\Big[\underset{\tau\to f}{\mathcal{F}}\{z(\tau)\,w(\tau-t)\}\Big]^*. \tag{2.7.2}$$

Taking the IFT ($f \to \tau$) of both sides gives

$$\begin{aligned} R_z(t,\tau) &= [z(\tau)\, w(\tau - t)] \underset{\tau}{*} [z^*(-\tau)\, w^*(-\tau - t)] \\ &= \int_{-\infty}^{\infty} z(\lambda)\, w(\lambda - t)\, z^*(\lambda - \tau)\, w^*(\lambda - \tau - t)\, d\lambda \\ &= \int_{-\infty}^{\infty} z(u + \tfrac{\tau}{2})\, w(u - t + \tfrac{\tau}{2})\, z^*(u - \tfrac{\tau}{2})\, w^*(u - t - \tfrac{\tau}{2})\, du \end{aligned} \tag{2.7.3}$$

where $\lambda = u + \frac{\tau}{2}$ is the dummy variable in the convolution. Exploiting the evenness of w, this can be written

$$\begin{aligned} R_z(t,\tau) &= \int_{-\infty}^{\infty} w^*(t - u + \tfrac{\tau}{2})\, w(t - u - \tfrac{\tau}{2})\, z(u + \tfrac{\tau}{2})\, z^*(u - \tfrac{\tau}{2})\, du \\ &= G(t,\tau) \underset{t}{*} K_z(t,\tau) \end{aligned} \tag{2.7.4}$$

where

$$G(t,\tau) = w^*(t + \tfrac{\tau}{2})\, w(t - \tfrac{\tau}{2}) \tag{2.7.5}$$

and $K_z(t,\tau)$ is given by Eq. (2.1.8). $G(t,\tau)$ is called the **time-lag kernel**.[6] Eq. (2.7.4) defines the time-lag kernel as that which must be convolved in time with the IAF to obtain the smoothed IAF; the word "smoothed" refers to the convolution. We shall adopt this definition for *all* TFDs given by Eq. (2.7.1).

Eq. (2.7.5) gives the time-lag kernel for the spectrogram. As w is real, we may interchange w and w^*, leading to the conclusion that the time-lag kernel for the spectrogram is simply the IAF of the observation window function.

2.7.2 Wigner-Ville Distribution

The "smoothed IAF" for the WVD is

$$R_z(t,\tau) = K_z(t,\tau) = \delta(t) \underset{t}{*} K_z(t,\tau) \tag{2.7.6}$$

so that

$$G(t,\tau) = \delta(t). \tag{2.7.7}$$

In this trivial case, the "smoothing" makes no difference.

2.7.3 Rihaczek Distribution

Eq. (2.6.3) may be written

$$\rho_z(t,f) = \underset{\tau \to f}{\mathcal{F}} \{ z(t)\, z^*(t - \tau) \}. \tag{2.7.8}$$

[6] The term "kernel" was used in this sense by Claasen and Mecklenbräuker [32]. To minimize the risk of confusion between the "time-lag kernel" $G(t,\tau)$ and the "signal kernel" $K_z(t,\tau)$, the latter is usually called the IAF in this book.

Taking the IFT gives

$$\begin{aligned} R_z(t,\tau) &= z(t)\, z^*(t-\tau) && (2.7.9)\\ &= \delta(t-\tfrac{\tau}{2}) \underset{t}{*} [z(t+\tfrac{\tau}{2})\, z^*(t-\tfrac{\tau}{2})] && (2.7.10)\\ &= \delta(t-\tfrac{\tau}{2}) \underset{t}{*} K_z(t,\tau) && (2.7.11) \end{aligned}$$

so that

$$G(t,\tau) = \delta(t-\tfrac{\tau}{2}). \qquad (2.7.12)$$

2.7.4 Levin Distribution

Using Eq. (2.7.8) as the definition of the Rihaczek distribution, and taking the real part, we obtain for the Levin distribution

$$\begin{aligned} \rho_z(t,f) &= \mathrm{Re}\left\{ \underset{\tau\to f}{\mathcal{F}} \{z(t)\, z^*(t-\tau)\} \right\} && (2.7.13)\\ &= \tfrac{1}{2} \underset{\tau\to f}{\mathcal{F}} \{z(t)\, z^*(t-\tau)\} + \tfrac{1}{2} \left[\underset{\tau\to f}{\mathcal{F}} \{z(t)\, z^*(t-\tau)\} \right]^*. && (2.7.14) \end{aligned}$$

Taking the IFT, we obtain

$$\begin{aligned} R_z(t,\tau) &= \tfrac{1}{2}\, z(t)\, z^*(t-\tau) + \tfrac{1}{2}\, z^*(t)\, z(t+\tau) && (2.7.15)\\ &= \tfrac{1}{2}\delta(t-\tfrac{\tau}{2}) \underset{t}{*} K_z(t,\tau) + \tfrac{1}{2}\delta(t+\tfrac{\tau}{2}) \underset{t}{*} K_z(t,\tau)\\ &= \tfrac{1}{2}[\delta(t+\tfrac{\tau}{2}) + \delta(t-\tfrac{\tau}{2})] \underset{t}{*} K_z(t,\tau) && (2.7.16) \end{aligned}$$

so that

$$G(t,\tau) = \tfrac{1}{2}[\delta(t+\tfrac{\tau}{2}) + \delta(t-\tfrac{\tau}{2})]. \qquad (2.7.17)$$

2.7.5 Windowed Rihaczek Distribution

Eq. (2.6.10) can be written

$$\begin{aligned} \rho_z(t,f) &= z(t) \underset{\tau\to f}{\mathcal{F}} \{z^*(-\tau)\, w^*(-\tau-t)\}\, e^{-j2\pi f t} && (2.7.18)\\ &= z(t) \underset{\tau\to f}{\mathcal{F}} \{z^*(t-\tau)\, w^*(-\tau)\}. && (2.7.19) \end{aligned}$$

Taking the IFT gives

$$\begin{aligned} R_z(t,\tau) &= z(t)\, z^*(t-\tau)\, w^*(-\tau) && (2.7.20)\\ &= [\delta(t-\tfrac{\tau}{2}) \underset{t}{*} K_z(t,\tau)]\, w^*(-\tau) && (2.7.21)\\ &= [w^*(-\tau)\, \delta(t-\tfrac{\tau}{2})] \underset{t}{*} K_z(t,\tau) && (2.7.22) \end{aligned}$$

so that

$$G(t,\tau) = w^*(-\tau)\, \delta(t-\tfrac{\tau}{2}). \qquad (2.7.23)$$

Because w is real and even, this reduces to

$$G(t,\tau) = w(\tau)\,\delta(t-\tfrac{\tau}{2}). \tag{2.7.24}$$

Comparing Eqs. (2.7.11) and (2.7.22), we see that the smoothed IAFs of the RD and the windowed RD differ by the factor $w^*(-\tau)$; that is, the distributions differ by a windowing operation in the lag domain prior to Fourier transformation from τ to f [31].

2.7.6 Windowed Levin Distribution

From Eq. (2.7.19), the real part of the windowed RD is

$$\tfrac{1}{2}\,z(t)\underset{\tau\to f}{\mathcal{F}}\{z^*(t-\tau)\,w^*(-\tau)\} \;+\; \tfrac{1}{2}\,z^*(t)\Big[\underset{\tau\to f}{\mathcal{F}}\{z^*(t-\tau)\,w^*(-\tau)\}\Big]^*. \tag{2.7.25}$$

Taking the IFT, we find that the smoothed IAF of the windowed LD is

$$\begin{aligned} R_z(t,\tau) &= \tfrac{1}{2}\,z(t)\,z^*(t-\tau)\,w^*(-\tau) + \tfrac{1}{2}\,z^*(t)\,z(t+\tau)\,w(\tau) \\ &= \tfrac{1}{2}\,[\delta(t-\tfrac{\tau}{2}) \underset{t}{*} K_z(t,\tau)]\,w^*(-\tau) + \tfrac{1}{2}\,[\delta(t+\tfrac{\tau}{2}) \underset{t}{*} K_z(t,\tau)]\,w(\tau) \\ &= \tfrac{1}{2}\,[w(\tau)\,\delta(t+\tfrac{\tau}{2}) + w^*(-\tau)\,\delta(t-\tfrac{\tau}{2})] \underset{t}{*} K_z(t,\tau) \end{aligned} \tag{2.7.26}$$

so that

$$G(t,\tau) = \tfrac{1}{2}\,[w(\tau)\,\delta(t+\tfrac{\tau}{2}) + w^*(-\tau)\,\delta(t-\tfrac{\tau}{2})] \tag{2.7.27}$$

or, because w is real and even,

$$G(t,\tau) = \tfrac{1}{2}\,w(\tau)\,[\delta(t+\tfrac{\tau}{2}) + \delta(t-\tfrac{\tau}{2})]. \tag{2.7.28}$$

Comparing Eqs. (2.7.16) and (2.7.26), and noting that w is real and even, we see that the smoothed IAFs of the LD and the windowed LD differ by the factor $w(\tau)$; that is, the distributions differ by a windowing operation in the lag domain [31].

2.7.7 Page Distribution

Rewriting Eq. (2.5.8) using the unit step function $u(t)$, we obtain for the Page distribution

$$\rho_z(t,f) = 2\,\mathrm{Re}\left\{\int_{-\infty}^{\infty} z^*(t)\,z(t-\lambda)\,u(\lambda)\,e^{j2\pi f\lambda}d\lambda\right\}. \tag{2.7.29}$$

With the substitution $\tau = -\lambda$, this becomes

$$\rho_z(t,f) = 2\,\mathrm{Re}\left\{\underset{\tau\to f}{\mathcal{F}}\{z^*(t)\,z(t+\tau)\,u(-\tau)\}\right\} \tag{2.7.30}$$

$$= \underset{\tau\to f}{\mathcal{F}}\{z^*(t)\,z(t+\tau)\,u(-\tau)\} \;+\; \Big[\underset{\tau\to f}{\mathcal{F}}\{z^*(t)\,z(t+\tau)\,u(-\tau)\}\Big]^*. \tag{2.7.31}$$

Taking the IFT, we obtain

$$\begin{aligned} R_z(t,\tau) &= z^*(t)\, z(t+\tau)\, u(-\tau) + z(t)\, z^*(t-\tau)\, u(\tau) && (2.7.32)\\ &= u(-\tau)[\delta(t+\tfrac{\tau}{2}) \underset{t}{*} K_z(t,\tau)] \;+\; u(\tau)[\delta(t-\tfrac{\tau}{2}) \underset{t}{*} K_z(t,\tau)] && (2.7.33)\\ &= [u(-\tau)\,\delta(t+\tfrac{\tau}{2}) + u(\tau)\,\delta(t-\tfrac{\tau}{2})] \underset{t}{*} K_z(t,\tau) && (2.7.34) \end{aligned}$$

so that

$$\begin{aligned} G(t,\tau) &= u(-\tau)\,\delta(t+\tfrac{\tau}{2}) + u(\tau)\,\delta(t-\tfrac{\tau}{2}) && (2.7.35)\\ &= \delta(t-|\tfrac{\tau}{2}|). && (2.7.36) \end{aligned}$$

2.7.8 Relationship between the WVD and Other TFDs

By taking the FT of Eq. (2.7.4) w.r.t. τ and using specific forms for $G(t,\tau)$, all the considered TFDs can be written in the same form as Eq. (2.2.15):

$$\rho_z(t,f) = \gamma(t,f) \underset{(t,f)}{**} W_z(t,f) \tag{2.7.37}$$

where

$$\gamma(t,f) = \underset{\tau\to f}{\mathcal{F}}\{G(t,\tau)\} \tag{2.7.38}$$

is the TFD time-frequency kernel.

This then suggests that all the TFDs naturally introduced so far can be considered to be smoothed WVDs. This observation led to the design or rediscovery of several other TFDs that are briefly discussed next.

2.7.9 Other Popular TFDs

Having derived some TFDs by intuitive methods and then determined their time-lag kernels, let us now define a few more TFDs directly in terms of their time-lag kernels.

Name	$G(t,\tau)$
Windowed WVD (w-WVD)	$\delta(t)\, w(\tau)$
Sinc *or* Born-Jordan (BJ)	$\frac{1}{\lvert 2\alpha\tau\rvert}\,\mathrm{rect}\,\frac{t}{2\alpha\tau}$
Exponential *or* Choi-Williams (CW)	$\frac{\sqrt{\pi\sigma}}{\lvert\tau\rvert} e^{-\pi^2\sigma t^2/\tau^2}$
Windowed sinc *or* Zhao-Atlas-Marks (ZAM)	$w(\tau)\,\mathrm{rect}\,\frac{t}{2\tau/a}$
B-distribution (BD)	$\lvert\tau\rvert^{\beta}\cosh^{-2\beta} t$
Modified B-distribution (MBD)	$\frac{\cosh^{-2\beta} t}{\int_{-\infty}^{\infty}\cosh^{-2\beta}\xi\, d\xi}$

In the above table, the parameters α, σ, a and β are real and positive, and $w(\tau)$ is a window function. The CW distribution was defined in [33] and the ZAM distribution

in [34]. The BJ distribution, called the "sinc distribution" in [28, p. 26], was defined in [7,35] using an operational rule of Born and Jordan [36, p. 873]. Observe that the BJ distribution is a special case of the ZAM with $a = 1/\alpha$ and $w(\tau) = a/|2\tau|$. These distributions are illustrated for a linear FM signal in Fig. 2.7.1, parts (f)–(i). The BD, w-WVD, and MBD kernels are "separable", while the w-WVD kernel is also "Doppler-independent" and the MBD kernel is also "lag-independent"; these concepts are discussed later, especially in Article 5.7. In Fig. 2.7.1 parts (j)–(l) we have respectively plotted a Doppler-independent, a lag-independent, and a separable-kernel TFD of a linear FM signal. We shall see [e.g. in Table 3.3.3 on p. 77] that the separable and Doppler (lag)-independent kernels have been introduced in order to obtain certain desired TFD properties.

For convenience, Table 2.7.1 collects and tabulates the definitions of the TFDs that have been derived heuristically in this chapter, and of the six TFDs that have just been defined in terms of their time-lag kernels.

2.8 Summary and Discussion

Constructing a quadratic TFD from the *analytic associate* of a given real signal, rather than from the signal itself, avoids spurious terms caused by interference between positive-frequency and negative-frequency components.

Every TFD that we have derived heuristically is *quadratic in the signal*; that is, if the signal is scaled by a factor k, the TFD is scaled by a factor k^2. This is to be expected because

(a) Each TFD considered so far is related to some sort of *energy density*. For example, the Page distribution is defined as a gradient of energy, hence accommodating for the negative values that occur in the TFD.

(b) The signal has been assumed to be an effort variable or a flow variable (examples of effort variables are voltage, force, and pressure; the corresponding flow variables are current, linear velocity, and volume velocity), *and* power is proportional to the product of an effort variable and the corresponding flow variable, hence (in a linear system) to the *square* of the effort variable or of the flow variable.

(c) We have seen in Section 2.7 that every TFD considered in this chapter can be written as the FT of a smoothed IAF [Eq. (2.7.1)], which is the convolution of an auxiliary function (the time-lag kernel filter $G(t,\tau)$) and the ordinary IAF $K_z(t,\tau)$, which in turn is *quadratic* in the signal.

Eq. (2.7.4) effectively defines a TFD in terms of its time-lag kernel and is the key to the theory and design of quadratic TFDs, as will be detailed in the next chapter.

References

[1] B. Boashash, "Estimating and interpreting the instantaneous frequency of a signal—Part 1: Fundamentals," *Proc. IEEE*, vol. 80, pp. 520–538, April 1992.

Table 2.7.1: Special forms of selected quadratic TFDs (3rd column), together with their time-lag kernels (2nd column). The window $w(\tau)$ is assumed to be real and even. Integrals, unless otherwise noted, are from $-\infty$ to ∞. The forms involving double integrals are obtained by direct substitution of the time-lag kernel into Eq. (3.2.9). The w-WVD may also be so obtained. Other forms are quoted from this chapter.

Distribution	$G(t,\tau)$	$\rho_z(t,f)$
Wigner-Ville	$\delta(t)$	$\int_{-\infty}^{\infty} z(t+\frac{\tau}{2})\, z^*(t-\frac{\tau}{2})\, e^{-j2\pi f\tau}\, d\tau$
Levin	$\frac{1}{2}\big[\delta(t+\frac{\tau}{2})+\delta(t-\frac{\tau}{2})\big]$	$\mathrm{Re}\big\{z(t)\, Z^*(f)\, e^{-j2\pi ft}\big\}$
Born-Jordan	$\frac{1}{\lvert 2\alpha\tau\rvert}\,\mathrm{rect}\,\frac{t}{2\alpha\tau}$	$\int_{-\infty}^{\infty}\int_{t-\lvert\alpha\tau\rvert}^{t+\lvert\alpha\tau\rvert} \frac{1}{2\alpha\tau}\, z(u+\frac{\tau}{2})\, z^*(u-\frac{\tau}{2})\, e^{-j2\pi f\tau}\, du\, d\tau$
Modified B	$\frac{\cosh^{-2\beta} t}{\int_{-\infty}^{\infty}\cosh^{-2\beta}\xi\, d\xi}$	$\iint \frac{\cosh^{-2\beta}(t-u)}{\int\cosh^{-2\beta}\xi\, d\xi}\, z(u+\frac{\tau}{2})\, z^*(u-\frac{\tau}{2})\, e^{-j2\pi f\tau}\, du\, d\tau$
w-WVD	$\delta(t)\, w(\tau)$	$\int_{-\infty}^{\infty} w(\tau)\, z(t+\frac{\tau}{2})\, z^*(t-\frac{\tau}{2})\, e^{-j2\pi f\tau}\, d\tau$
w-Levin	$\frac{w(\tau)}{2}\big[\delta(t+\frac{\tau}{2})+\delta(t-\frac{\tau}{2})\big]$	$\mathrm{Re}\Big\{z(t)\,\Big[\int_{-\infty}^{\infty} z(\tau)\, w(\tau-t)\, e^{-j2\pi f\tau}\, d\tau\Big]^*\, e^{-j2\pi ft}\Big\}$
ZAM	$w(\tau)\,\mathrm{rect}\,\frac{t}{2\tau/a}$	$\int_{-\infty}^{\infty}\int_{t-\lvert\frac{\tau}{a}\rvert}^{t+\lvert\frac{\tau}{a}\rvert} w(\tau)\, z(u+\frac{\tau}{2})\, z^*(u-\frac{\tau}{2})\, e^{-j2\pi f\tau}\, du\, d\tau$
Rihaczek	$\delta(t-\frac{\tau}{2})$	$z(t)\, Z^*(f)\, e^{-j2\pi ft}$
w-Rihaczek	$w(\tau)\,\delta(t-\frac{\tau}{2})$	$z(t)\,\Big[\int_{-\infty}^{\infty} z(\tau)\, w(\tau-t)\, e^{-j2\pi f\tau}\, d\tau\Big]^*\, e^{-j2\pi ft}$
Page	$\delta(t-\lvert\frac{\tau}{2}\rvert)$	$\frac{\partial}{\partial t}\Big[\Big\lvert\int_{-\infty}^{t} z(\tau)\, e^{-j2\pi f\tau}\, d\tau\Big\rvert^2\Big]$
Choi-Williams	$\frac{\sqrt{\pi\sigma}}{\lvert\tau\rvert}e^{-\pi^2\sigma t^2/\tau^2}$	$\iint \frac{\sqrt{\pi\sigma}}{\lvert\tau\rvert}e^{\frac{-\pi^2\sigma(t-u)^2}{\tau^2}}\, z(u+\frac{\tau}{2})\, z^*(u-\frac{\tau}{2})\, e^{-j2\pi f\tau}\, du\, d\tau$
B	$\lvert\tau\rvert^{\beta}\cosh^{-2\beta} t$	$\iint \frac{\lvert\tau\rvert^{\beta}}{\cosh^{2\beta}(t-u)}\, z(u+\frac{\tau}{2})\, z^*(u-\frac{\tau}{2})\, e^{-j2\pi f\tau}\, du\, d\tau$
Spectrogram	$w(t+\frac{\tau}{2})\, w(t-\frac{\tau}{2})$	$\Big\lvert\int_{-\infty}^{\infty} z(\tau)\, w(\tau-t)\, e^{-j2\pi f\tau}\, d\tau\Big\rvert^2$

[2] B. Boashash, P. J. O'Shea, and M. J. Arnold, "Algorithms for instantaneous frequency estimation: A comparative study," in *Proc. SPIE: Advanced Signal-Processing Algorithms, Architectures, and Implementations*, vol. 1348, pp. 126–148, Soc. of Photo-optical Instrumentation Engineers, San Diego, 10–12 July 1990.

[3] E. P. Wigner, "On the quantum correction for thermodynamic equilibrium," *Physics Review*, vol. 40, pp. 749–759, June 1932.

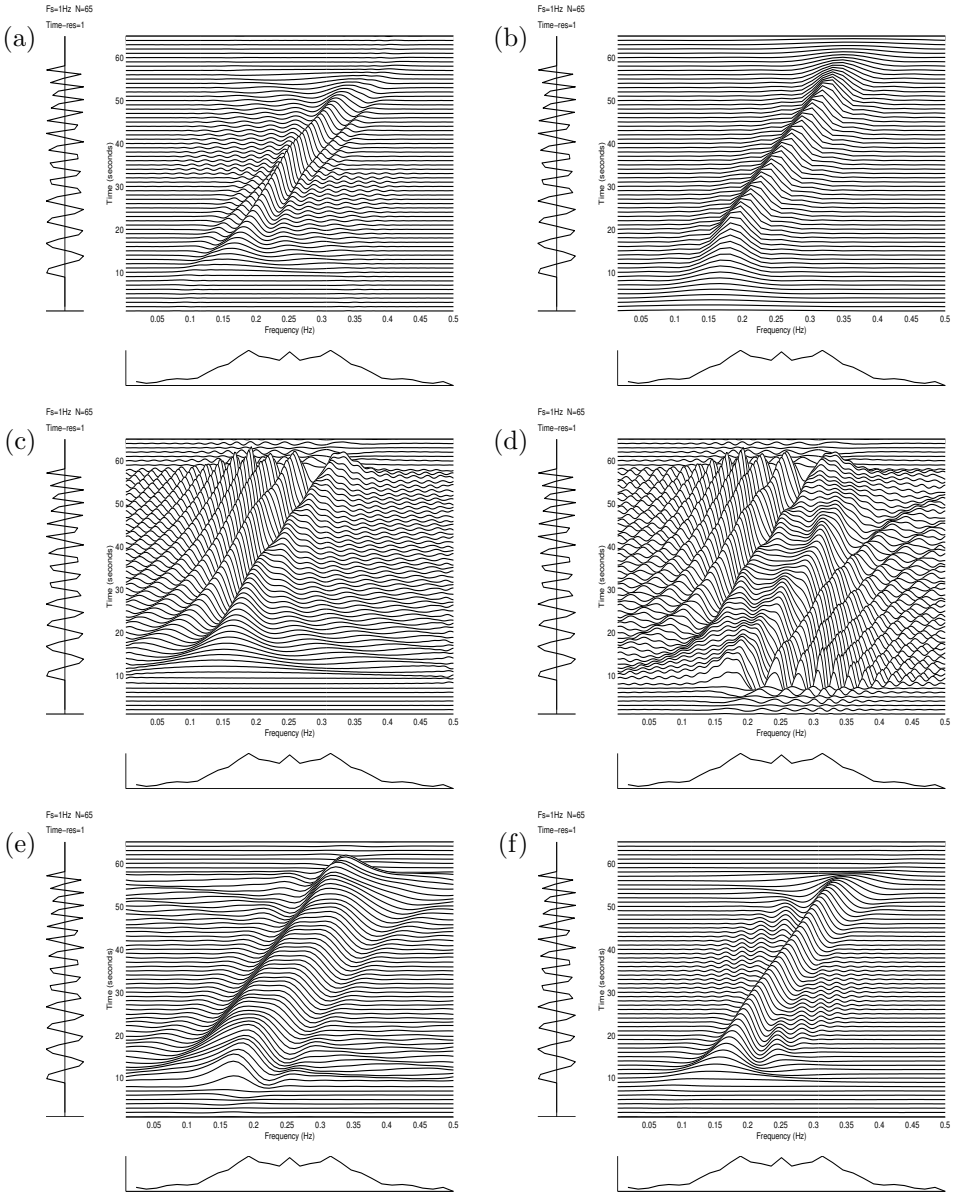

Fig. 2.7.1: TFDs of a linear FM signal with displayed duration 65 samples (sampling rate 1 Hz), unit amplitude from sample 9 to sample 57, zero amplitude elsewhere, frequency range 0.1 (at sample 1) to 0.4 (at sample 65): (a) Wigner-Ville; (b) Spectrogram, 21-point rectangular window; (c) Page; (d) Levin; (e) Windowed Levin, 19-point Hamming window; (f) Choi-Williams, $\sigma = 4$;... [continued].

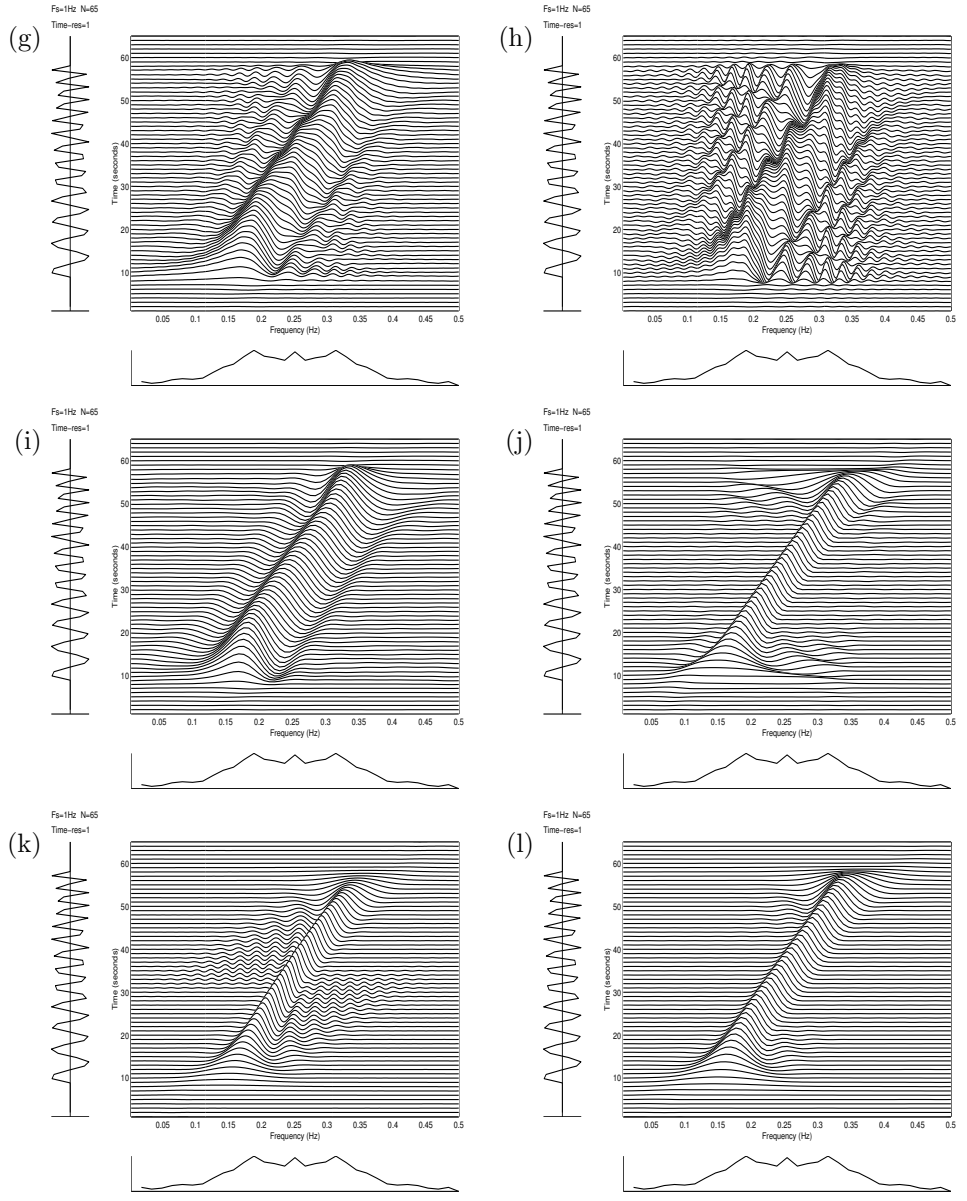

Fig. 2.7.1: [continuing] ...(g) Born-Jordan, $\alpha = 1/2$; (h) Zhao-Atlas-Marks, $a = 2$, $g_2(\tau) = 1$; (i) Zhao-Atlas-Marks, $a = 2$, $g_2(\tau) = 19$-point Hamming window; (j) Doppler-independent, $g_2(\tau) = 29$-point Hamming window; (k) Lag-independent, $g_1(t) = 9$-point Hanning; (l) Separable kernel, $g_1(t) = 9$-point Hanning, $g_2(\tau) = 29$-point Hamming.

[4] S. D. Conte and C. de Boor, *Elementary numerical analysis: An algorithmic approach*. Tokyo: McGraw-Hill, 3rd ed., 1980.

[5] B. Boashash, "Note on the use of the Wigner distribution for time-frequency signal analysis," *IEEE Trans. Acoustics, Speech, & Signal Processing*, vol. 36, pp. 1518–1521, September 1988.

[6] J. Ville, "Théorie et applications de la notion de signal analytique," *Cables et Transmissions*, vol. 2A, no. 1, pp. 61–74, 1948. In French. English translation: I. Selin, *Theory and applications of the notion of complex signal*, Rand Corporation Report T-92 (Santa Monica, CA, August 1958).

[7] L. Cohen, "Time-frequency distributions—A review," *Proc. IEEE*, vol. 77, pp. 941–981, July 1989. Invited paper.

[8] B. Boashash and P. J. Black, "An efficient real-time implementation of the Wigner-Ville distribution," *IEEE Trans. Acoustics, Speech, & Signal Processing*, vol. 35, pp. 1611–1618, November 1987.

[9] B. Boashash and H. J. Whitehouse, "High resolution Wigner-Ville analysis," in *Eleventh GRETSI Symp. on Signal Processing and its Applications*, pp. 205–208, Nice, France, 1–5 June 1987.

[10] H. J. Whitehouse, B. Boashash, and J. M. Speiser, "High-resolution processing techniques for temporal and spatial signals," in *High-resolution methods in underwater acoustics* (M. Bouvet and G. Bienvenu, eds.), ch. 4, pp. 127–176, Berlin: Springer, 1991.

[11] W. Martin, "Time-frequency analysis of random signals," in *Proc. IEEE Internat. Conf. on Acoustics, Speech and Signal Processing (ICASSP'82)*, vol. 3, pp. 1325–1328, Paris, 3–5 May 1982.

[12] D. Gabor, "Theory of communication," *J. IEE*, vol. 93(III), pp. 429–457, November 1946.

[13] G. R. Putland and B. Boashash, "Can a signal be both monocomponent and multicomponent?," in *Third Australasian Workshop on Signal Processing Applications (WoSPA 2000)*, Brisbane, Australia, 14–15 December 2000. Paper no. 32.

[14] W. Koenig, H. K. Dunn, and L. Y. Lacy, "The sound spectrograph," *J. Acoustical Soc. of America*, vol. 18, no. 1, pp. 19–49, 1946.

[15] J. Imberger and B. Boashash, "Application of the Wigner-Ville distribution to temperature gradient microstructure: A new technique to study small-scale variations," *J. of Physical Oceanography*, vol. 16, pp. 1997–2012, December 1986.

[16] L. R. O. Storey, "An investigation of whistling atmospherics," *Phil. Trans. Roy. Soc.*, vol. A246, pp. 113–141, 1953.

[17] B. Boashash, "Time-frequency signal analysis," in *Advances in Spectrum Analysis and Array Processing* (S. Haykin, ed.), vol. 1, ch. 9, pp. 418–517, Englewood Cliffs, NJ: Prentice-Hall, 1991.

[18] D. L. Jones and T. W. Parks, "A high-resolution data-adaptive time-frequency representation," *IEEE Trans. Acoustics, Speech, & Signal Processing*, vol. 38, pp. 2127–2135, December 1990.

[19] M. K. Emresoy and A. El-Jaroudi, "Iterative instantaneous frequency estimation and adaptive matched spectrogram," *Signal Processing*, vol. 64, pp. 157–65, January 1998.

[20] J. Kay and R. Lerner, *Lectures in Communications Theory.* McGraw-Hill, 1961.

[21] C. W. Helstrom, "An expansion of a signal in Gaussian elementary signals," *IEEE Trans. Information Theory*, vol. 12, pp. 81–82, January 1966.

[22] I. Daubechies, "The wavelet transform: A method for time-frequency localization," in *Advances in Spectrum Analysis and Array Processing* (S. Haykin, ed.), vol. 1, ch. 8, pp. 366–417, Englewood Cliffs, NJ: Prentice-Hall, 1991.

[23] Y. Meyer, *Wavelets: Algorithms and applications.* Philadelphia, PA: Soc. for Industrial and Applied Mathematics, 1993. Translated and revised by Robert D. Ryan. Original French title: *Ondelettes et algorithems concurrents.*

[24] S. G. Mallat, *A Wavelet Tour of Signal Processing.* San Diego / London: Academic Press, 2nd ed., 1999.

[25] C. H. Page, "Instantaneous power spectra," *J. of Applied Physics*, vol. 23, pp. 103–106, January 1952.

[26] A. W. Rihaczek, "Signal energy distribution in time and frequency," *IEEE Trans. Information Theory*, vol. 14, pp. 369–374, May 1968.

[27] J. G. Kirkwood, "Quantum statistics of almost classical ensembles," *Physics Review*, vol. 44, pp. 31–37, 1933.

[28] L. Cohen, "Introduction: A primer on time-frequency analysis," in *Time-Frequency Signal Analysis: Methods and Applications* (B. Boashash, ed.), ch. 1, pp. 3–42, Melbourne/N.Y.: Longman-Cheshire/Wiley, 1992.

[29] M. J. Levin, "Instantaneous spectra and ambiguity functions," *IEEE Trans. Information Theory*, vol. 10, pp. 95–97, January 1964.

[30] H. Margenau and R. N. Hill, "Correlation between measurements in quantum theory," *Progress of Theoretical Physics*, vol. 26, pp. 722–738, 1961.

[31] G. R. Putland. personal communications, Signal Processing Research Centre, Queensland University of Technology, 2001.

[32] T. A. C. M. Claasen and W. F. G. Mecklenbräuker, "The Wigner Distribution—A tool for time-frequency signal analysis; Part 3: Relations with other time-frequency signal transformations," *Philips J. of Research*, vol. 35, no. 6, pp. 372–389, 1980.

[33] H.-I. Choi and W. J. Williams, "Improved time-frequency representation of multicomponent signals using exponential kernels," *IEEE Trans. Acoustics, Speech, & Signal Processing*, vol. 37, pp. 862–871, June 1989.

[34] Y. Zhao, L. E. Atlas, and R. J. Marks II, "The use of cone-shaped kernels for generalized time-frequency representations of non-stationary signals," *IEEE Trans. Acoustics, Speech, & Signal Processing*, vol. 38, pp. 1084–1091, July 1990.

[35] L. Cohen, "Generalized phase-space distribution functions," *J. of Mathematical Physics*, vol. 7, pp. 781–786, May 1966.

[36] M. Born and P. Jordan, "Zur quantenmechanik," *Zeitschrift für Physik.*, vol. 34, pp. 858–888, 1925.